STATISTICS, OPTIMIZATION AND INFORMATION COMPUTING
Stat., Optim. Inf. Comput., Vol. **x**, Month 2024, pp 0–10.
Published online in International Academic Press (www.IAPress.org)

A Generalized Backstepping Controller Design for a Second-Order Magnetic Levitation System

Oscar Danilo Montoya [1], Walter Gil-González [2], Adolfo Andrés Jaramillo-Matta [1]

[1] *Facultad de Ingeniería, Universidad Distrital Francisco José de Caldas, Bogotá D.C. 110121, Colombia*
[2] *Departament de Ingeniería Eléctrica, Facultad de Ingenierías, Universidad Tecnológica de Pereira, Pereira 660003, Colombia.*

Abstract This research addresses the challenge of stabilizing a second-order magnetic levitation system through a nonlinear control approach. The proposed controller is rooted in backstepping control theory, which ensures the asymptotic convergence of the system's incremental state variables to the origin through a Lyapunov-based framework. A key advantage of this method is the generalized control input, expressed in polynomial form with four adjustable control gains, which enables precise tuning to achieve the desired dynamic performance. A major contribution of this study is the formal demonstration of stable performance provided by the generalized controller in second-order dynamic systems, with a particular emphasis on its application in magnetic levitation. Numerical simulations in Matlab/Simulink showcase the controller's effectiveness across three different sets of control gains, allowing the system to provide critically damped, overdamped, and underdamped dynamic responses with respect to the desired position of the levitating metallic mass.

Keywords Backstepping control design, generalized control law, magnetic levitation system, stability test, time-domain simulation

AMS 2010 subject classifications 62J07

DOI:10.19139/soic-2310-5070-2164

1. Introduction

1.1. General context

Nonlinear systems control is a critical field in engineering and science as the complex behaviors involved challenge traditional linear control methods [1]. Nonlinear systems are prevalent in various fields, including robotics, aerospace, and all branches of engineering, where precise control is essential for ensuring stability and achieving adequate dynamic performance under varying operating conditions [2].

Magnetic levitation systems (MLS) are among the most classical nonlinear dynamic systems used for testing advanced control methodologies [3]. This type of system utilizes magnetic forces to suspend objects without physical contact, thereby exemplifying various challenges [4]. The nonlinear dynamics associated with magnetic forces significantly complicate their control design. Effective control is essential to prevent instability and ensure the reliable operation of magnetic levitation technologies in practical applications [5].

1.2. Motivation

The increasing complexity of modern engineering systems necessitates advanced control strategies that can effectively manage nonlinear dynamics [6]. MLS, utilized in high-speed transportation [7], precision manufacturing

*Correspondence to: O. D. Montoya (Email: odmontoyag@udistrital.edu.co). Facultad de Ingeniería, Universidad Distrital Francisco José de Caldas, Bogotá D.C. 110121, Colombia.

ISSN 2310-5070 (online) ISSN 2311-004X (print)

[8], and medical devices [9], attest to the demand for such sophisticated control mechanisms. The inherent nonlinearities in magnetic levitation, particularly the magnetic forces that fluctuate with position and velocity, pose significant challenges to achieving stable and efficient control [3].

Backstepping control design has emerged as a powerful method for addressing the complexities of nonlinear systems [10]. Its recursive structure facilitates the systematic breakdown of control problems, making it particularly effective in applications such as MLS, which require precise and robust control strategies [11]. This research explores the synergy between backstepping control design and MLS, aiming to enhance the stability, performance, and practical implementation of these cutting-edge technologies.

1.3. Literature review

Magnetically levitating metallic masses have been widely analyzed in literature. This subsection presents some relevant works on this topic.

The authors of [3] proposed a novel MLS using the real-time control Simulink feature of the SIMLAB microcontroller. The system's control was validated through simulations and experiments, exhibiting superiority over conventional strategies. Three controllers –*i.e.*, a linear quadratic regulator (LQR), the proportional-integral-derivative (PID), and lead compensation— were compared based on parameters such as peak overshoot, settling time, and rise time. The LQR reported the best performance, with a peak overshoot of 14.6%, a settling time of 0.199 seconds, and a rise time of 0.064 seconds, proving its stability and effectiveness.

In [4], a robust proportional-derivative gain-scheduling controller (PD-GS-C) for an unstable MLS with two electromagnets was presented. The system's nonlinearity required advanced control techniques, which is why a nonlinear state-space model was derived and linearized around five operating points. The PD controller gains were determined using a parameter space technique, while big bang-big crunch optimization further refined them. The controller's performance was evaluated based on overshoot, settling time, and rise time. MATLAB simulations and experiments confirmed the PD-GS-C's effectiveness in stabilizing the system.

The work by [12] designed an optimized PID controller to regulate the ball position of an MLS. The electromagnetic force in the MLS was controlled by sensing the ball's position using infrared sensors. System performance was improved in both the time and frequency domains by optimizing the PID controller parameters using the grey wolf optimizer. This algorithm tuned the parameters while minimizing performance indices such as the integral time-weighted absolute error (ITAE) and the integral time-weighted square error (ITSE). The effectiveness of the proposed controller was validated by comparing it against classical tuning methods.

The study by [13] presented a control approach for a MLS using exact feedback linearization. The system's nonlinear dynamics were analyzed via the Euler-Lagrange method and transformed into a linear equivalent. MATLAB simulations showed that the controlled output accurately followed the desired reference.

The authors of [14] addressed the challenge of large-displacement magnetic levitation actuation and stability in non-liquid environments by proposing a system with an active levitation mode. The system ensured uniform force and reduced overshoot using dual electromagnetic actuators for a superimposed magnetic field as well as dual Hall sensors for displacement measurement. A neural network-based PID controller automatically tuned the parameters, enhancing adaptability and solving tracking performance deterioration issues. Strong robustness and stability were achieved during both ascending and descending motions.

The work by [15] focused on the modeling and control of an MLS, developing a nonlinear model for a specific region while accounting for gravity compensation. A control strategy based on the concept of *passivity* was designed, equating the levitation system to a passive one and implementing a position regulation approach. Real-time experiments were conducted to validate the performance of the proposed control scheme.

Additional control approaches for MLS include the use of artificial neural networks [16], sliding mode control combined with integral backstepping [17], fuzzy logic controllers [18], and Lyapunov-based methods [19], among others.

1.4. Contributions and scope

Considering the above-presented literature review regarding the existing control methods applied to MLS, this research presents the following contributions:

i. A generalization of the backstepping control design applied to a second-order class of nonlinear dynamic systems.
ii. A polynomial control law that ensures the asymptotic stabilization of a MLS during closed-loop operation in the sense of Lyapunov.

It is important to note that, within the scope of this research, the following considerations have been made: (i) the third-order dynamic model of the MLS is simplified into a second-order model, wherein the control input corresponds to the current flowing through the system's inductor; and (ii) it is assumed that all system parameters are known and free from any uncertainties. In applying backstepping control to the MLS, the key difference between the approach proposed in this research and the methods reported in [17] lies in our focus on the second-order dynamic model of the MLS. Our study introduces a general polynomial control law with four control gains, allowing for flexible tuning to achieve the desired ball position, including damped, underdamped, and overdamped behaviors. This approach differs from the integral versions of backstepping control discussed in the referenced works.

1.5. Document structure

The remainder of this document is organized as follows. Section 2 presents the general theory of backstepping control design applied to second-order dynamical systems, including the corresponding stability analysis. Section 3 details the dynamical modeling of the second-order MLS, covering the state-variable representation, and the incremental dynamical modeling. Section 4 discusses the application of backstepping control to the MLS and demonstrates its stability, and Section 5 presents the numerical validations carried out for different control parameter configurations. Finally, Section 6 summarizes the main conclusions of this research and suggests potential directions for future work.

2. Backstepping control theory

Backstepping control theory is a structured and iterative approach used in control engineering. It is particularly well-suited for stabilizing nonlinear systems in strict feedback form [10]. This technique systematically breaks down complex control tasks into smaller, more manageable sub-problems, allowing for the step-by-step construction of control laws and the development of Lyapunov functions at each stage. The Lyapunov function is meticulously selected to ensure system stability, and its derivative is made negative-definite by carefully designing the control inputs. Backstepping is especially useful for nonlinear systems and can be extended to handle cases whose system parameters are unknown or vary over time by integrating parameter estimation methods into the framework. This approach provides a robust and systematic method for designing stabilizing controllers across a broad spectrum of nonlinear systems.

2.1. General system form

A controller design using backstepping control theory facilitates the analysis of the nonlinear system dynamics described by Equations (1) and (2) while preserving generality in the approach.

$$\dot{\eta} = f(\eta) + g(\eta)\,\zeta, \tag{1}$$

$$\dot{\zeta} = h(\eta, \zeta) + j(\eta, \zeta)\,u. \tag{2}$$

In these equations, η and ζ represent the state variables, where $f(\eta)$ and $h(\eta, \zeta)$ are smooth nonlinear functions describing the system's intrinsic dynamics. The terms $g(\eta)$ and $j(\eta, \zeta)$ correspond to the control input matrices that connect the state variables to the control inputs, enabling the design of a control law that stabilizes the system.

2.2. Controller design

To design a backstepping controller that asymptotically stabilizes the Dynamical System (1)–(2) around the origin, the following assumptions are made:

Assumption 1 (Existence of the inverse function)
The structure of the nonlinear matrix $j(\eta,\zeta)$ allows for the existence of the inverse function $j^{-1}(\eta,\zeta)$, such that $j(\eta,\zeta)\,j^{-1}(\eta,\zeta)=1$.

Assumption 2 (Candidate Lyapunov function)
There is a candidate Lyapunov function $\mathcal{V}(x)$ that satisfies the following conditions:

1. $\mathcal{V}(x)$ is positive-definite, meaning that $\mathcal{V}(x)>0$ for all $x\neq 0$, and $\mathcal{V}(0)=0$.
2. The derivative $\dot{\mathcal{V}}(x)$ is negative-definite, *i.e.*, $\dot{\mathcal{V}}(x)<0$.

Considering Assumptions 1 and 2, the general backstepping control design is defined below.

Lemma 1 (Control input)
The dynamical system defined by (1) and (2) is asymptotically stabilized at the origin with a general control input u that takes the following form:

$$u=j^{-1}(\eta,\zeta)\left(-k_p\zeta+k_p\varphi(\eta)-\frac{\partial\mathcal{V}}{\partial\eta}g(\eta)+\frac{\partial\varphi}{\partial\eta}\left(f(\eta)+g(\eta)\,\zeta\right)-h(\eta,\zeta)\right). \tag{3}$$

where $\varphi(\eta)$ is a design function defined based on the structure of the functions $f(\eta)$ and $g(\eta)$, and k_p is a positive proportional control gain.

Proof

To demonstrate that the control input u defined in (3) asymptotically stabilizes the Dynamical System (1)–(2), Assumption 3 is required.

Assumption 3 (Existence of a positive-definite function)
The time derivative of the Lyapunov candidate function $\mathcal{V}(x)$, *i.e.*, $\dot{\mathcal{V}}(x)$ satisfies the following condition:

$$\dot{\mathcal{V}}(x)\leq-\mathcal{W}(x), \tag{4}$$

where $\mathcal{W}(x)$ is a positive-definite function.

Now, if the control input u in (3) is substituted into Equation (2), the following result is obtained:

$$\dot{\zeta}=-k_p\left(\zeta-\varphi(\eta)\right)-\frac{\partial\mathcal{V}}{\partial\eta}g(\eta)+\frac{\partial\varphi}{\partial\eta}\left(f(\eta)+g(\eta)\,\zeta\right). \tag{5}$$

Note that an auxiliary variable z can be defined as $\zeta-\varphi(\eta)$, which allows defining the following augmented Lyapunov candidate function $\mathcal{H}(\eta,\zeta)$:

$$\mathcal{H}(\eta,z)=\mathcal{V}(\eta)+\frac{1}{2}z^2, \tag{6}$$

which has the following time derivative function:

$$\begin{aligned}\dot{\mathcal{H}}(\eta,z)=&\dot{\mathcal{V}}(\eta)+z\dot{z},\\ =&\dot{\mathcal{V}}(\eta)+\left(\zeta-\varphi(\eta)\right)\left(\dot{\zeta}-\dot{\varphi}(\eta)\right),\\ =&\dot{\mathcal{V}}(\eta)+\left(\zeta-\varphi(\eta)\right)\left(\dot{\zeta}-\frac{\partial\varphi}{\partial\eta}\dot{\eta}\right).\end{aligned} \tag{7}$$

Now, the Dynamical System (1)–(5) is substituted into (7), which yields the following:

$$\begin{aligned}\dot{\mathcal{H}}(\eta,z)=&\dot{\mathcal{V}}(\eta)+\left(\zeta-\varphi(\eta)\right)\left(-k_p\left(\zeta-\varphi(\eta)\right)-\frac{\partial\mathcal{V}}{\partial\eta}g(\eta)+\frac{\partial\varphi}{\partial\eta}\left(f(\eta)+g(\eta)\,\zeta\right)-\frac{\partial\varphi}{\partial\eta}\left(f(\eta)+g(\eta)\,\zeta\right)\right),\\ =&\dot{\mathcal{V}}(\eta)+\left(\zeta-\varphi(\eta)\right)\left(-k_p\left(\zeta-\varphi(\eta)\right)-\frac{\partial\mathcal{V}}{\partial\eta}g(\eta)\right),\\ =&\dot{\mathcal{V}}(\eta)-k_p\left(\zeta-\varphi(\eta)\right)^2-\left(\zeta-\varphi(\eta)\right)\frac{\partial\mathcal{V}}{\partial\eta}g(\eta).\end{aligned} \tag{8}$$

Here, considering the definition provided by the authors of [10] regarding backstepping control design, the selection of the auxiliary control input $\zeta = \varphi(\eta)$ is as follows:

$$\begin{aligned}\dot{\mathcal{H}}(\eta, z) =& \frac{\partial \mathcal{V}}{\partial \eta}\dot{\eta} - k_p(\zeta - \varphi(\eta))^2 - (\zeta - \varphi(\eta))\frac{\partial \mathcal{V}}{\partial \eta}g(\eta), \\ =& \frac{\partial \mathcal{V}}{\partial \eta}(f(\eta) + g(\eta)\zeta) - k_p(\zeta - \varphi(\eta))^2 - (\zeta - \varphi(\eta))\frac{\partial \mathcal{V}}{\partial \eta}g(\eta), \\ =& \frac{\partial \mathcal{V}}{\partial \eta}(f(\eta) + g(\eta)\varphi(\eta)) - k_p(\zeta - \varphi(\eta))^2. \end{aligned} \tag{9}$$

Note that, if $\varphi(\eta)$ is selected as the state variable ζ, then the following is obtained:

$$\dot{\mathcal{H}}(\eta, z) \leq -\mathcal{W}(\eta) - k_p(\zeta - \varphi(\eta))^2 < 0, \tag{10}$$

which confirms that the control input defined in (3) asymptotically stabilizes the Dynamical System (1)–(2) around the origin of coordinates, thus completing the proof.

□

Note that the backstepping control method is particularly well-suited for MLS due to its effectiveness in handling nonlinear dynamics [10]. Unlike other control methods, backstepping allows for the systematic design of controllers for systems with complex, nonlinear behavior, as is the case of the second-order dynamics of MLS [19]. Additionally, backstepping provides a clear framework for ensuring stability in the sense of Lyapunov, making it highly advantageous for achieving asymptotic stability during closed-loop operation [17]. This control method also offers flexibility in addressing uncertainties and disturbances, which are common in practical MLS applications, providing robust performance compared to conventional methods such as PID or linear feedback control [10].

3. MLS modeling

This section presents the dynamical model of the MLS. Additionally, it explores the transformation of this model into an equivalent state variable representation, defines the equilibrium point, and analyzes the error dynamics.

3.1. Mathematical modeling

Figure 1 depicts the schematic representation of an MLS, where F_{mag} represents the magnetic force associated with the current flow i through the inductor L; F_{g} corresponds to the gravitational force acting on the metal mass m; R represents the equivalent resistance effect on the inductor; v is the input voltage; and e represents the equivalent voltage measured through the Hall effect [3].

To obtain the dynamical model of the MLS, Newton's laws of motion are applied, which yields

$$m\ddot{y} = F_{\text{g}} - F_{\text{mag}}. \tag{11}$$

Remark 1
The formulation of the equivalent magnetic force varies across different studies. This work considers the model provided by the authors of [3], representing the magnetic force applied to the metallic ball as cubic regarding the distance and linear in the case of the current.

$$F_{\text{mag}} = k_{\text{mag}}\left(\frac{1}{y^3}\right)i, \tag{12}$$

with k_{mag} being a constant related to the electromagnet's turn ratio and cross-sectional area.

Now, considering the definition of the magnetic force in (12), and the gravitational force (*i.e.*, $F_{\text{g}} = mg$) in Equation (11), the following dynamical model is obtained:

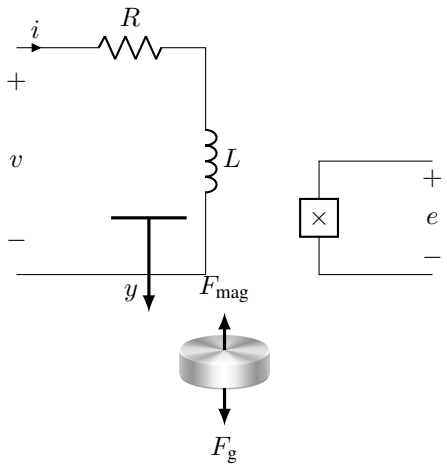

Figure 1. Schematic representation of a MLS

$$m\ddot{y} = mg - k_{\text{mag}} \left(\frac{1}{y^3} \right) i, \tag{13}$$

Remark 2
The dynamical model of the MLS neglects the dynamics of the inductor by assuming the recommendations of [3], where i is considered as the control input for the mechanical part of this system.

It is worth mentioning that our selection of a second-order model for the MLS, instead of the classical third-order model, was based on the following considerations:

i. **Computational efficiency:** The second-order model reduces the computational load in comparison with the third-order one. This is essential for real-time control applications, where fast response times are critical, particularly in MLS, whose dynamics can change rapidly [20].
ii. **Accuracy:** The second-order model sufficiently captures the key dynamic behaviors, *e.g.*, the oscillations and settling times, commonly seen in MLS. Higher-order terms often provide diminishing returns in terms of accuracy while adding complexity [3].
iii. **Simplified control design:** Second-order models are easier to control and stabilize. Their reduced complexity allows for more straightforward control strategies that ensure system stability, particularly when managing levitation height and force dynamics in MLS [21].
iv. **Easier parameter identification:** Parameter estimation is simpler in second-order models, making it easier to tune the system in real-world scenarios, where measurement noise may affect higher-order models [22].
v. **Established precedents:** Various research works, including [3], have demonstrated that second-order models can accurately describe the essential dynamics of MLS without requiring the additional complexity of third-order models.

3.2. *State variable representation and equilibrium point*

To represent the dynamical model of the MLS in (13), the following state variables are defined: $\eta = y - y_\star$, $\zeta = \dot{y}$, and the control input $\omega = i$, which yields the following equivalent dynamical system:

$$\dot{\eta} = \zeta, \tag{14}$$

$$\dot{\zeta} = g - \left(\frac{k_{\text{mag}}}{m}\right)\left(\frac{1}{(\eta + y_\star)^3}\right)\omega, \tag{15}$$

where $y_\star$ is the desired operating point of the metallic mass, implying that $\eta_\star = 0$.

Remark 3
Note that, in order to calculate the equilibrium point, it is assumed that the desired position of the metallic mass (*i.e.*, $y_1^\star$) is known. This implies that, under steady-state conditions, $\dot{\eta} = 0$ and $\dot{\zeta} = 0$, which yields

$$\zeta_\star = 0, \tag{16}$$

$$\omega_\star = \left(\frac{mg}{k_{\text{mag}}}\right)(y_\star)^3. \tag{17}$$

3.3. *Incremental model*

The application of backstepping control requires the dynamical system to have an equilibrium point at the origin of coordinates. To this effect, the incremental model is used. The structure of the control input ω is defined as follows:

$$\omega = (\eta + y_\star)^3 \left(\frac{m}{k_{\text{mag}}}\right)(g - u), \tag{18}$$

where u is an auxiliary control input that regulates the state variables. Note that, by substituting Equation (18) into (15), the following incremental model is reached:

$$\dot{\eta} = \zeta, \tag{19}$$

$$\dot{\zeta} = u. \tag{20}$$

Remark 1
The main idea of the backstepping controller design is to obtain the structure of the control input u that asymptotically stabilizes the Incremental Model (19)-(20) via the general structure defined by (5).

4. Backstepping control applied to the MLS

This section presents the general backstepping control input to stabilize the second-order MLS. In addition, the general structure of $\mathcal{W}(\eta)$ is obtained in order to confirm Assumption 3.

4.1. *Control input design*

The backstepping design requires the identification of the functions in (1)–(2) through a comparison with the incremental model in (19)–(20). This yields the following results:

$$\begin{aligned} f(\eta) &= 0, \\ g(\eta) &= 1, \\ h(\eta, \zeta) &= 0, \\ h(\eta, \zeta) &= 1. \end{aligned} \tag{21}$$

In addition, the structure of $\varphi(\eta)$ is defined, as well as the initial candidate Lyapunov function $\mathcal{V}(\eta)$:

$$\varphi(\eta) = -\alpha\eta^{2n-1}, \tag{22}$$

$$\mathcal{V}(\eta) = \frac{1}{2}\beta\eta^{2n}, \tag{23}$$

with α and β being two positive-definite constants and n a positive integer number.

Now, the partial derivatives of the functions $\varphi(\eta)$ and $\mathcal{V}(\eta)$ are then obtained:

$$\frac{\partial\varphi}{\partial\eta} = -(2n-1)\alpha\eta^{2(n-1)}, \tag{24}$$

$$\frac{\partial\mathcal{V}}{\partial\eta} = n\beta\eta^{2n-1}, \tag{25}$$

Finally, the General Control Input (5) to stabilize the Incremental Model (19)–(20) takes the following structure:

$$u = -k_p\left(\zeta + \alpha\eta^{2n-1}\right) - n\beta\eta^{2n-1} - (2n-1)\alpha\eta^{2(n-1)}\zeta. \tag{26}$$

Remark 2

Note that the general control input ω, as defined by (18), becomes a general control input for stabilizing the MLS (14)–(15) when the backstepping control input (26) is substituted into it, which yields the following:

$$\omega = (\eta + y_\star)^3\left(\frac{m}{k_{\text{mag}}}\right)g + (\eta + y_\star)^3\left(\frac{m}{k_{\text{mag}}}\right)\left(k_p\left(\zeta + \alpha\eta^{2n-1}\right) + n\beta\eta^{2n-1} + (2n-1)\alpha\eta^{2(n-1)}\zeta\right), \tag{27}$$

It is worth mentioning that, at the equilibrium point (*i.e.*, $\eta_\star = 0$ and $\zeta_\star = 0$), the General Control Input (27) is reduced to (17), which is the control input at the equilibrium point.

4.2. Finding the $\mathcal{W}(\eta)$ function

To determine the structure of $\mathcal{W}(\eta)$, $\zeta = \varphi(\eta)$ is defined, and the time derivative of the initial candidate Lyapunov function in (23) is taken, resulting in

$$\begin{aligned}\dot{\mathcal{V}}(\eta) &= n\beta\eta^{2n-1}\dot{\eta},\\ &= n\beta\eta^{2n-1}\left(f(\eta) + g(\eta)\zeta\right),\\ &= -n\beta\eta^{2n-1}\alpha\eta^{2n-1},\\ &= -n\alpha\beta\eta^{2(2n-1)} \leq \mathcal{W}(\eta).\end{aligned} \tag{28}$$

Here, it is evident that $\mathcal{W}(\eta)$ can be selected as follows:

$$\mathcal{W}(\eta) = n\alpha\beta\eta^{\gamma(2n-1)}, \tag{29}$$

which clearly is a positive-definite function for the appropriate selection of the positive constant γ.

5. Numerical validation

To validate the effective performance of the proposed generalized backstepping controller and its application to the second-order MLS, simulation parameters were obtained from [3]. These parameters include operating and current limits, the equivalent metallic mass, and the magnetic force constant, among others. All these parameters are listed in Table 1.

Three parameter combinations were analyzed to evaluate the performance of the proposed backstepping control design. The studied parameters are listed in Table 2. Note that, in all parameter combinations, n has been selected as 1 since it corresponds to a linear control input in Equation (26).

Table 1. Parameters of the MLS

Parameter	Value	Unit	Parameter	Value	Unit	Parameter	Value	Unit
k_{mag}	2.40×10^{-6}	$\text{kgm}^{45}/\text{s}^2\text{A}$	$y_\star$	$20{\times}10^{-3}$	m	$i_{\min}$	0	A
m	0.02985	kg	$i_\star$	0.9758	A	$i_{\max}$	4	A

Table 2. Control gain parameters for the simulations

Case	α	β	k_p	n
I	5	6	20	1
II	10	1250	8	1
III	6	7	2	1

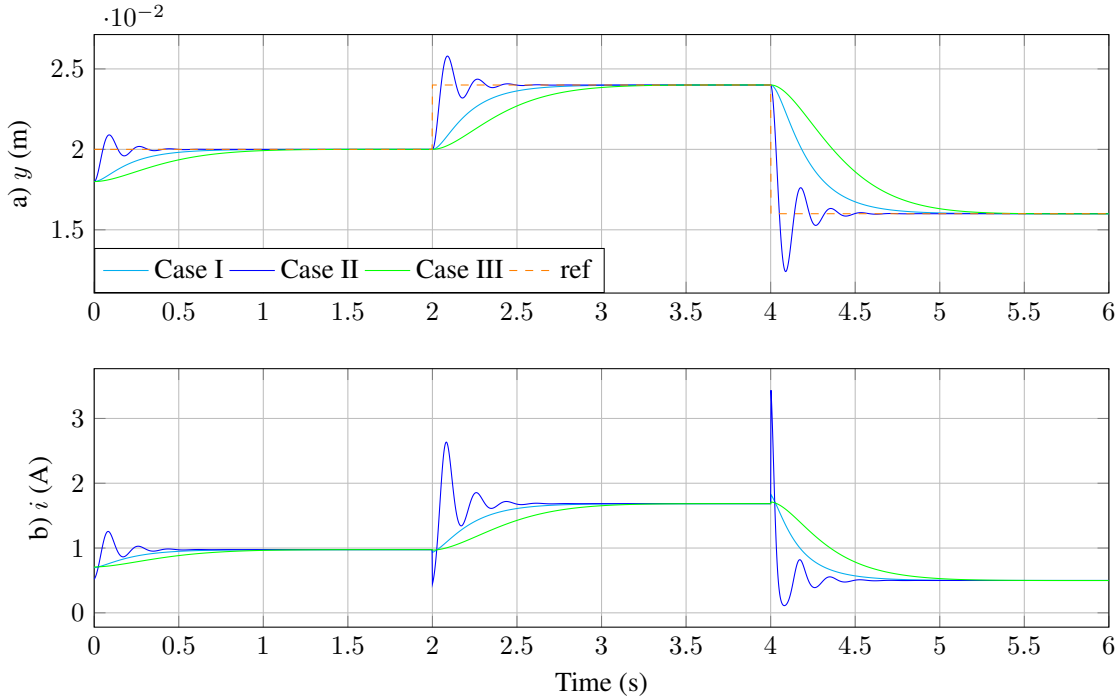

Figure 2. Position of the levitating metallic mass

Figure 2 illustrates the dynamic behavior of the metallic mass for three position references and their effect on the control input's performance: from 0 to 2 seconds, $y_\star = 20$ mm; from 2 to 4 seconds, $y_\star = 24$ mm; and, from 4 to 6 seconds, $y_\star = 16$ mm.

The dynamic behavior of the metallic mass and the current input depicted in Figure 2 allows stating the following:

i. The three control parameter combinations asymptotically stabilize the magnetic ball's position around the desired reference (see Figure 2a). In Case I, the system exhibits a critically damped behavior, whereas, in Case II, it resembles an underdamped system. Finally, in Case III, the position of the metallic mass also behaves as an underdamped dynamical system.

ii. The control input associated with the inductor current reaches three equilibrium points (see Figure 2b), which depend on the desired reference position of the metallic mass (*i.e.*, $y_\star$), as shown in Equation (17). The equilibrium points for the current input are as follows: $i_\star = 0.9758$ A between 0 and 2 seconds; $i_\star = 1.6862$ A between 2 and 4 seconds; and $i_\star = 0.4996$ A between 4 and 6 seconds.

iii. The main result regarding the control input is that, regardless of the analyzed case, it remains within its upper and lower bounds (*i.e.*, between 0 and 4 A). However, the most significant control challenges arise in Case

II, where the current peak is higher than those of Cases I and III. Additionally, the behavior of the control signal highlights the non-minimum phase characteristics of the second-order dynamical model representing the MLS.

To determine which of the simulation cases featured a better performance, three classical indices were analyzed (Table 3): the integral time square error (ITSE), the integral absolute error (IAS), and the integral time absolute error (ITAE). Table 3 also presents the average stabilization times.

Table 3. Summary of the analyzed indices

Case	ITSE	IAE	ITAE	T_s [s]
I	4.096×10^{-5}	3.302×10^{-3}	1.008×10^{-2}	1.2
II	1.008×10^{-5}	1.067×10^{-3}	0.316×10^{-2}	0.7
III	8.304×10^{-5}	5.904×10^{-3}	1.863×10^{-2}	1.4

Regarding the indices and stabilization times presented in Table 3, the following can be stated:

i. The stabilization times indicate that, in Case III (overdamped control gain parametrization), the metallic mass takes longer to reach the desired reference, *i.e.*, approximately 1.4 seconds, which is twice the time reported for Case II (underdamped parametrization). In the critically damped case, the stabilization time falls between the aforementioned scenarios, taking around 1.2 seconds to reach the desired reference.
ii. The performance indices show that the best parametrization corresponds to Case II, the underdamped scenario. Although the system exhibits oscillations around the reference, they quickly diminish, allowing the system to efficiently reach the desired reference.

6. Conclusions and future work

This research designed a nonlinear controller for a second-order MLS using backstepping control theory. The proposed controller approach is general and took a polynomial structure with four control gains that allows selecting the desired system performance as a function of the operational requirements and physical constraints associated with the control input's lower and upper bounds.

Numerical simulations with three different control gain combinations demonstrated the expected performance of the levitating metallic mass position concerning asymptotic stabilization.. However, the behavior of the dynamic response reported damped, underdamped, and overdamped performances, demonstrating the importance of adequate control parameters selection.

The generalization of the backstepping controller for a second-order dynamical system demonstrated that the generalized control input enables the asymptotic convergence of the controlled variable with various time-domain performances. This poses a challenge for researchers in determining the most effective strategy for tuning control parameters in order to achieve the desired dynamic performance, emphasizing the nonlinear relationship between these parameters and the expected behavior of the metallic mass position.

As future work, the following areas could be explored: (i) the application of an optimization methodology to tune the control parameters that minimizes stabilization times while maintaining a first-order-like behavior; (ii) the proposal of new controllers for the second-order nonlinear equivalent model of the MLS, ensuring stability and addressing parameter uncertainties; and (iii) a comparison of the existing models for MLS, particularly concerning the magnetic force model.

Acknowledgments

The first author would like to thank the Master's program in Mathematics Teaching of Universidad Tecnológica de Pereira and the GCEM research group of Universidad Distrital Francisco José de Caldas. The authors acknowledge the support provided by Thematic Network 723RT0150, *Red para la integración a gran escala de energías*

renovables en sistemas eléctricos (RIBIERSE-CYTED), funded by the 2022 call for thematic networks of the CYTED (Ibero-American Program of Science and Technology for Development). This research was also supported by project no. 6-24-9, titled *Desarrollo de una metodología de control secundario para microrredes de corriente continua aisladas empleando control predictivo basado en el modelo*, under Universidad Tecnológica de Pereira's Vicerrectoría de Investigación, Innovación y Extensión.

REFERENCES

1. C. De Persis and P. Tesi. Learning controllers for nonlinear systems from data. *Annual Reviews in Control*, 56:100915, 2023.
2. Jenq-Lang Wu. Stabilizing controllers design for switched nonlinear systems in strict-feedback form. *Automatica*, 45(4):1092–1096, April 2009.
3. Mundher H.A. Yaseen and Haider J. Abd. Modeling and control for a magnetic levitation system based on SIMLAB platform in real time. *Results in Physics*, 8:153–159, March 2018.
4. Moayed Almobaied, Hassan S. Al-Nahhal, and Khaled B.A. Issa. Robust-pid controller design for magnetic levitation system using parameter space approach. *World Journal of Advanced Engineering Technology and Sciences*, 8(2):135–151, March 2023.
5. Wang Yang, Fanwei Meng, Man Sun, and Kai Liu. Passivity-based control design for magnetic levitation system. *Applied Sciences*, 10(7):2392, April 2020.
6. Mohammed Chadli, Sofiane Bououden, Salim Ziani, and Ivan Zelinka. *Advanced Control Engineering Methods in Electrical Engineering Systems*. Springer International Publishing, 2019.
7. Fengxing Li, Yougang Sun, Junqi Xu, Zhenyu He, and Guobin Lin. Control methods for levitation system of ems-type maglev vehicles: An overview. *Energies*, 16(7):2995, March 2023.
8. Lei Zhou and Jingjie Wu. Magnetic levitation technology for precision motion systems: A review and future perspectives. *International Journal of Automation Technology*, 16(4):386–402, July 2022.
9. Betul Karakuzu, Muge Anil İnevi, E. Alperay Tarim, Oyku Sarigil, Meltem Guzelgulgen, Seren Kecili, Selin Cesmeli, Sadik Koc, M. Semih Baslar, Ceyda Oksel Karakus, Engin Ozcivici, and H. Cumhur Tekin. Magnetic levitation-based miniaturized technologies for advanced diagnostics. *Emergent Materials*, July 2024.
10. Oscar Danilo Montoya-Giraldo, Carlos Alberto Ramírez-Vanegas, and Fernando Mesa. A phase-portrait stability analysis for a reaction wheel pendulum using a generalized backstepping control approach. *Statistics, Optimization & Information Computing*, Aug. 2024.
11. Jianping Cai, Changyun Wen, Hongye Su, and Zhitao Liu. Robust adaptive backstepping control of second-order nonlinear systems with non-triangular structure uncertainties. *IFAC Proceedings Volumes*, 47(3):10814–10819, 2014.
12. Shekhar Yadav, S.K. Verma, and S.K. Nagar. Optimized pid controller for magnetic levitation system. *IFAC-PapersOnLine*, 49(1):778–782, 2016.
13. Rudi Uswarman, Adha Imam Cahyadi, and Oyas Wahyunggoro. Control of a magnetic levitation system using feedback linearization. In *2013 International Conference on Computer, Control, Informatics and Its Applications (IC3INA)*, volume 3, pages 95–98. IEEE, November 2013.
14. Guancheng Liu, Yonghua Lu, Jiajun Xu, Zhanxiang Cui, and Haibo Yang. Magnetic levitation actuation and motion control system with active levitation mode based on force imbalance. *Applied Sciences*, 13(2):740, January 2023.
15. M. Velasco-Villa, R. Castro-Linares, and L. Corona-Ramirez. Modeling and passivity based control of a magnetic levitation system. In *Proceedings of the 2001 IEEE International Conference on Control Applications (CCA'01) (Cat. No.01CH37204)*, CCA-01, pages 64–69. IEEE, 2001.
16. M. Aliasghary, M. Aliyari Shoorehdeli, A. Jalilvand, and M. Teshnehlab. Magnetic levitation control based-on neural network and feedback error learning approach. In *2008 IEEE 2nd International Power and Energy Conference*, volume 1567, pages 1426–1430. IEEE, December 2008.
17. Hafiz Muhammad Salman Yaseen, Syed Ahmad Siffat, Iftikhar Ahmad, and Ali Shafiq Malik. Nonlinear adaptive control of magnetic levitation system using terminal sliding mode and integral backstepping sliding mode controllers. *ISA Transactions*, 126:121–133, July 2022.
18. A.K. Ahmad, Z. Saad, M.K Osman, I.S. Isa, S. Sadimin, and S.S. Abdullah. Control of magnetic levitation system using fuzzy logic control. In *2010 Second International Conference on Computational Intelligence, Modelling and Simulation*, pages 51–56. IEEE, September 2010.
19. Yichuan Wang, Danfeng Zhou, Jie Li, Mengxiao Song, and Qing Yang. Integral backstepping and lyapunov calm control design for magnetic levitation system. In *2021 40th Chinese Control Conference (CCC)*, volume 92, pages 674–678. IEEE, July 2021.
20. Katsuhiko Ogata. *Modern Control Engineering*. Prentice Hall PTR, USA, 2nd edition, 2010.
21. Ion Boldea and Syed A. Nasar. *Electric Drives*. CRC Press, September 2016.
22. Karl Johan Astrom and Richard M. Murray. *Feedback Systems: An Introduction for Scientists and Engineers*. Princeton University Press, USA, 2008.